Journal of Building Technology, 2025, Volume 7, Issue 1
DOI: 10.32629/jbt.v7i1.3689
ISSN Online: 2717-5103
ISSN Print: 2705-1390

Geogrids - An Option for the Reinforcement of Soft Soils Under Reinforced Concrete Structures

Michael Sam Giler-Sánchez, Jean Alejandro Macías-García, Evangelos Manouris, Marguith-Yanira Espín León

Universidad Técnica de Manabí, Portoviejo, Ecuador.

Abstract: Construction professionals are at the forefront in reinforcing the soil with the use and application of methods and materials that help increase its bearing capacity, since one of the main causes of building collapse and settlement is soft soil. For this study, a five-story reinforced concrete building was designed using structural software and a soil-structure interaction analysis was performed. Immediate and differential settlements were calculated with the application of loads from the structure. Four reinforcement analysis models were considered: 1) without improvement; 2) with soil replacement; 3) with geogrids; and 4) with geogrids and footing width reduction. The bearing capacity was estimated using data from soil studies and material parameters from quarries near the study area in Portoviejo, Ecuador. An adaptation to the formulas of Meyerhof & Hanna was applied for the soil substitution alternative, while the formulas of Huang & Meng were used and applied for the geogrids. The aim of this analysis is to obtain a high bearing capacity value of the soil that leads to savings in foundation material and at the same time to achieve low numbers of settlements that are deduced to the safety of the structure. The results of the reinforcement in relation to the natural soil revealed a considerable increase for the geogrid alternatives compared to soil substitution, and a reduction in settlements. The percentages obtained after analysis and calculations demonstrate the benefits of using geogrids under this type of structure.

Key words: geogrid; foundations; bearing capacity; settlement; reinforcement

1. Introduction

According to IEE & MAGAP (2012), Portoviejo is a canton with variable geomorphology, located in the central part of the coastal region of Manabí, Ecuador. This area is notable for the disappearance of the coastal mountain range, represented by some hills that descend to a central plain, and for the fine soil formations present in several areas below the hills. The central part of the territory is the lowest-lying area, characterized by the crossing of the Portoviejo River from south-southwest to north-northwest, and its channels pose a high level of flood hazard (IEE & MAGAP, 2012).

Seismic zoning studies carried out in the city of Portoviejo by the National Polytechnic School (2017) reflect that the urban areas of the city are considered soft soils with a high liquefaction potential, classified according to the NEC-SE-DS as Type D, E and F soils. Soft soils are characterized by geotechnical problems such as low to very low compressive strength and foundation settlements (González de Vallejo, 2002).

Geogrids are geosynthetic materials formed by parallel and perpendicular ribs connected to each other with openings that allow the passage of soil (Koerner, 2005). They are resistant to soil degradation processes, due to being a chemically

and biologically inert material, and to ensure their quality they must resist tearing, wear and punching (MTOP, 2013). The main function of geogrids is reinforcement; being rigid and having wide enough openings, they allow an interconnection with the adjacent soil or rock, to reinforce or segregate both materials (Das, 2011). Their use creates a geogrid-soil interaction that increases resistance by receiving, transmitting and distributing loads towards the soil evenly, achieving an improvement (Latha and Somwanshi, 2009). Geogrids have been increasingly used in road projects due to their positive financial impacts, reduced earthwork thickness, and increased pavement lifespan (Sarmiento, 2017). For these reasons, this study addressed their use for soil reinforcement under loads produced by a reinforced concrete building designed with shallow foundations and strip footings. A detailed analysis was conducted, including the calculation, evaluation, and subsequent comparison of soil replacement alternatives and the use of geogrids.

The soil-structure interaction method is a mathematical model that distributes springs using the ballast modulus or modulus of elasticity beneath the footings as if they were grids with elastic supports to simulate the soil (Bernal, 2005). Based on this method, the vertical loads were calculated, and the immediate and differential settlements produced by the building were quantified.

2. Materials and Methods

2.1 Study area

The chosen study area is georeferenced at latitude 1° 1' 43.33" S and longitude 80° 28' 54.57" W, with an altitude of 31 m above sea level. It is located in the El Negrital sector of the 18 de Octubre parish in Portoviejo, Ecuador (See Figure 1), where the soil mechanics studies were conducted. This study area was chosen because it has similar characteristics to the central urban areas of Portoviejo, such as plastic clayey or silty soils with a water table very close to the surface and a soft consistency (Alvarado, 2018).

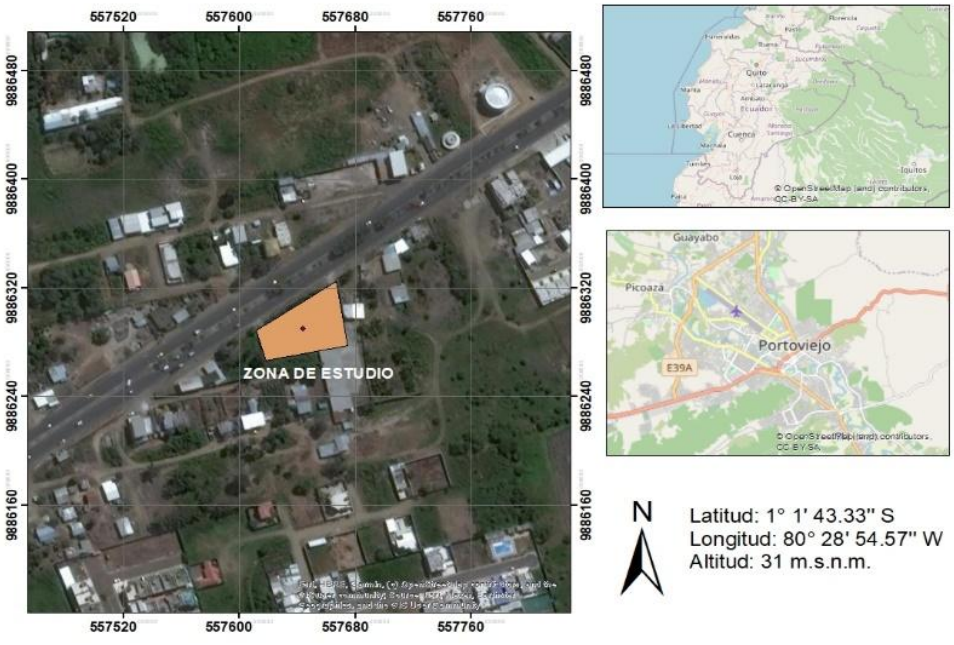

Figure 1. Study area.

2.2 Soil studies

Three SPT (Standard Penetration Test) probes were conducted at a depth of six meters to determine the soil stratigraphic profile, including soil classification, water table, and SPT impacts (See Figure 2).

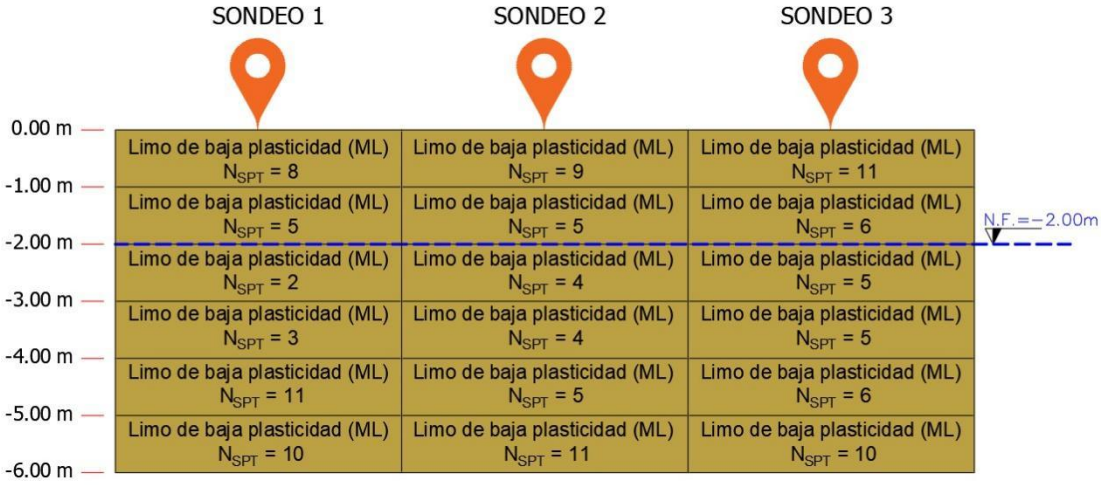

Figure 2. Soil stratigraphic profile.

Table 1. Parameters of saturated silty soil

Properties	Parameters
Specific weight (γ)	15.49 kN/m^3
Effective cohesion (c')	29.42 kPa
Effective friction angle (Ø')	0°

2.3 Structural design

A five-story residential reinforced concrete structure was designed, measuring 8.40 meters wide and 11.50 meters long. It consisted of beams, columns, solid slabs, and a foundation of seven continuous footings with a base offset (D_f) of 0.80 meters and a footing width (B) of 1.20 meters. The first four levels are single-family apartments, and the top floor is used as a laundry and event or meeting area. The structural elements, dead loads, and live loads of the structure were pre-designed according to the current Ecuadorian Construction Regulations (MIDUVI, 2014a, 2014b) and modeled in ETABS 20 structural software (See Figure 3).

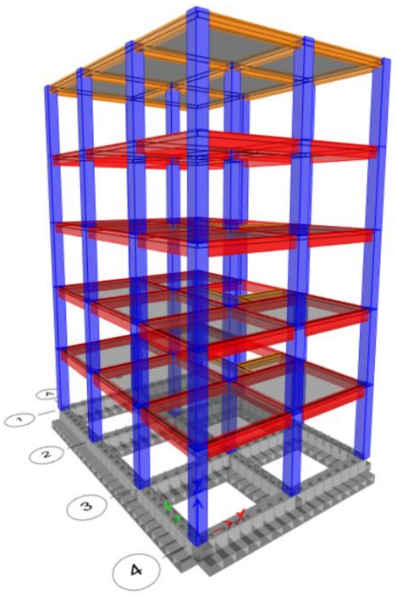

Figure 3. 3D view of the study building.

2.4 Soil replacement

To counteract the effects of the water table and soil moisture, a 50 cm layer of granular material (> 100 mm in diameter) known as Piedra Bola (Rock Rock) was placed. This layer will prevent the potential swelling of the saturated silt and provide a solid support base for the foundation. Above the Piedra Bola layer, a second 50 cm layer of gravel-sand material known as a Class III sub-base will be placed. This material will serve a dual purpose: sealing the Piedra Bola (Rock Rock) and filtering precipitation water. Therefore, the same material will be added above the footing (Df).

The Class III sub-base is made up of coarse aggregates obtained by sieving gravel or rocks that are mixed with crushed material or sand, with 30% to 70% of the material passing sieve No. 4 and no more than 20% passing sieve No. 200 (MTOP, 2013). The two improvement strata have an extra width of 50 cm. Figure 4 shows a graphic diagram of the section and plan with the improvement alternative with soil replacement.

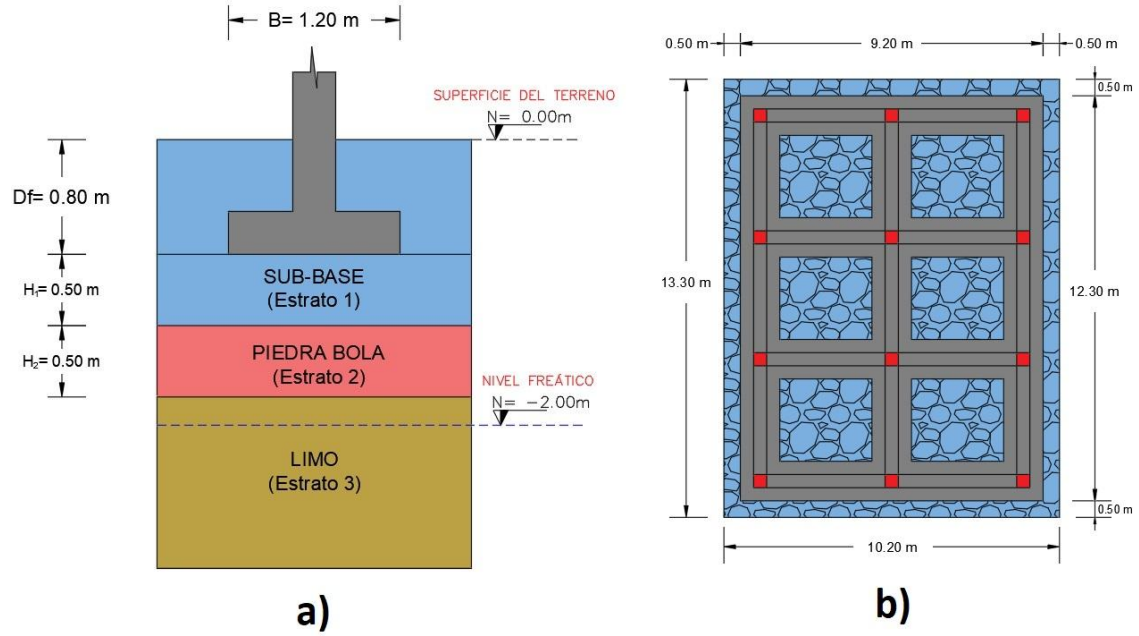

Figure 4. a) Section diagram and b) Plan diagram with soil replacement alternative.

Table 2 below presents the properties of the granular and sand-gravel materials used to replace the soil for each stratum.

Table 2. Properties of materials for soil replacement

Properties	Stone ball	Sub-base
Specific weight (γ)	13.83 kN/m³	18.64 kN/m³
Effective cohesion (c')	0 kPa	0 kPa
Angle of friction effective (Ø')	40°	40°

2.5 Meyerhof & Hanna's theory and its adaptation to the pragmatics of study

Using the formulas from the theory of Meyerhof & Hanna (1978), cited in Das (2014), the bearing capacity beneath the footings was calculated using the soil replacement alternative. These formulas were adapted to the three different strata. The nomenclature of the stratum properties is shown in Table 3.

Table 3. Nomenclature of soil replacement strata

Soil properties			
Stratum	Specific weight	Angle of friction	Cohesion
Sub-base	$\gamma_{(1)}$	$Ø'_{(1)}$	$C'_{(1)}$
Stone Ball	$\gamma_{(2)}$	$Ø'_{(2)}$	$C'_{(2)}$
Silt	$\gamma_{(3)}$	$Ø'_{(3)}$	$C'_{(3)}$

The bearing capacity calculation procedure using the soil replacement alternative was divided into two cycles:

1) Strong stratum (rock ball) over weak stratum (silt)

2) Strong stratum (sub-base) over weak stratum (rock ball)

The adaptation formulas of Meyerhof & Hanna's (1978) theory will be valid, if there are three continuous strata below the footing, with the upper stratum being stronger than the lower stratum. Furthermore, stratum 1 must continue from below the footing to the surface (D_f).

Cycle 1: Strong stratum (ball stone) over weak stratum (silence)

The adaptation of the bearing capacity equation of the weak stratum (Silt) consisted of adding the influence of the thickness and properties of stratum 1 to the confinement component of equation 1.

$$q_{b1}=c'_{(3)}\ N_{c(3)}\ F_{cs(3)}+(\gamma_{(1)}(D_f+H_1)+\gamma_{(2)}\ (H_2))\ N_{q(3)}\ F_{qs(3)}+1/2\ \gamma_{(3)}\ BN\gamma_{(3)}\ F_{\gamma s(3)} \quad \text{eq.1}$$

Where:

q_{b1} = Bearing capacity of the weak stratum (silt)

$Nc_{(3)}$, $N_{q(3)}$, $N_{\gamma(3)}$ = Bearing capacity factors for stratum 3 (silt)

$F_{cs(3)}$, $F_{qs(3)}$, $F_{\gamma s(3)}$ = Shape factors for stratum 3 (silt)

D_f = Footing offset

H_1 = Thickness of stratum 1 (sub-base) below the footing

H_2 = Thickness of stratum 2 (rock ball)

B = Width of the footing

Similarly, the bearing capacity of the strong stratum (rock ball) was adapted by adding the influence of the thickness and properties of stratum 1 to the confinement component of equation 2.

$$q_{t1}=c'_{(2)}\ N_{c(2)}\ F_{cs(2)}+(\gamma_{(1)}(D_f+H_1))\ N_{q(2)}\ F_{qs(2)}+1/2\ \gamma_{(2)}\ BN\gamma_{(2)}\ F_{\gamma s(2)} \quad \text{eq.2}$$

Where:

q_{t1} = Bearing capacity of the strong stratum (Rocky rock)

$N_{c(2)}$, $N_{q(2)}$, $N_{\gamma(2)}$ = Bearing capacity factors of stratum 2 (Rocky rock)

$F_{cs(2)}$, $F_{qs(2)}$, $F_{\gamma s(2)}$ = Shape factors of stratum 2 (Rocky rock)

The adaptation of the ultimate bearing capacity of Cycle 1 was based on adding the influence of the thickness of stratum 1 and is defined as (See equation 3):

$$q_{u1}=q_{b1}+\left(1+\frac{B}{L}\right)\left(\frac{2c'_a H_2}{B}\right)+\gamma_{(2)}\ (H_2)^2\ \left(1+\frac{B}{L}\right)\left(1+\frac{2\ (D_f+H_1)}{H_2}\right)\left(\frac{K_s\ \tan\phi'_{(2)}}{B}\right)-\gamma_{(2)}\ H_2 \leq q_{t1} \quad \text{eq.3}$$

Where:

q_{u1} = Ultimate load capacity of Cycle 1

L = Footing length

c'_a = Soil adhesive strength represented by the cohesion of layer 2 (Rock)

k_s = Punching shear coefficient

The ratio of the foundation width to the foundation length tends to zero when dealing with a continuous footing; therefore, B/L = 0 will be considered in the calculations.

Cycle 2: Strong stratum (sub-base) over weak stratum (ball stone)

To ensure continuity of bearing capacity in the calculation of the three strata, the weak stratum of Cycle 2 (q_{b2}) will be equal to the ultimate bearing capacity of Cycle 1 (q_{u1}), represented as (See equation 4):

$$q_{b2} = q_{u1} \quad \text{eq.4}$$

The load capacity of the strong stratum for Cycle 2 (Sub-base) is determined with the original equation of Meyerhof & Hanna (See equation 5):

$$q_{t2}=c'_1 N_{c(1)} F_{cs(1)}+\gamma_{(1)} D_f N_{q(1)} F_{qs(1)} +\frac{1}{2}\gamma_{(1)} B N_{\gamma(1)} F_{\gamma s(1)} \quad \text{eq.5}$$

Where:

q_{t2} = Bearing capacity of the strong stratum (sub-base)

$N_{c(1)}$, $N_{q(1)}$, $N_{\gamma(1)}$ = Bearing capacity factors for stratum 1 (sub-base)

$F_{cs(1)}$, $F_{qs(1)}$, $F_{\gamma s(1)}$ = Shape factors for stratum 1 (sub-base)

The equation for the ultimate bearing capacity of Cycle 2 is the one that will act below the footing and is defined by the Meyerhof & Hanna equation (See equation 6).

$$q_{u2}=q_{b2}+\left(1+\frac{B}{L}\right)\left(\frac{2c'_a H_1}{B}\right)+\gamma_{(1)} (H_1)^2 \left(1+\frac{B}{L}\right)\left(1+\frac{2D_f}{H_1}\right)\left(\frac{K_s \tan\phi'_{(1)}}{B}\right)-\gamma_{(1)} H_1 \leq q_{t2} \quad \text{eq.6}$$

Where:

q_{u2} = Ultimate load capacity of Cycle 2

L = Footing length

c'_a = Soil adhesive strength represented by the cohesion of layer 1 (sub-base)

K_s = Punching shear coefficient

$\phi'_{(1)}$ = Angle of friction of layer 1 (sub-base)

2.6 Geogrids

Two layers of square biaxial geogrids were used, separated into 30 cm thick layers. Due to the commercial width of the geogrid rolls, which is 3.90 meters, three rows of geogrids were required, with a 60 cm overlap and a 65 cm overwidth.

The confinement material is sandy and continues above the footing to the surface (D_f) to ensure good water drainage during periods of heavy rainfall. Figure 5 shows a graphical section and plan view of the geogrid improvement alternative.

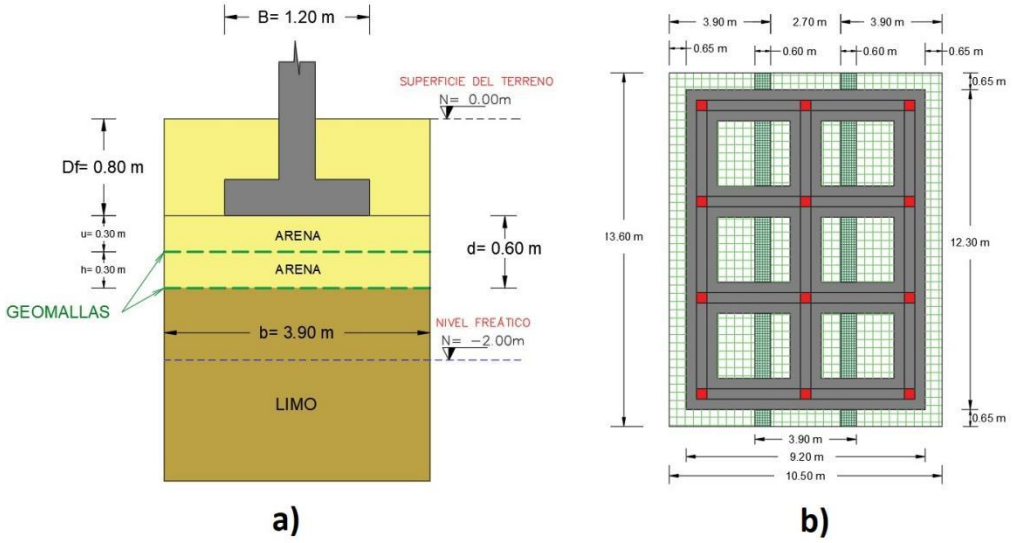

Figure 5. a) Section diagram and b) Plan view with geogrid alternative.

The geogrid parameters are considered: rib width (w) equal to 3 mm and rib spacing (W) equal to 40 mm. Regarding the properties corresponding to the granular confinement material (sand), we have a specific weight (γ) equal to 15.21 kN/m^3 and an effective friction angle ϕ' equal to 33°.

2.7 Huang & Meng theory

For geogrid calculations, we propose using the theory of Huang & Meng (1997), cited in Das (2009), since the formulas are valid for calculations with sandy soils and strip footings. The ultimate bearing capacity of the soil reinforced with geogrids (q_u) is represented as (see equation 7):

$$q_U=[0.5-0.1(\frac{B}{L})](B+2d*\tan\beta)\ \gamma\ N_\gamma+\gamma\ (D_f+d)\ N_q \quad \text{eq.7}$$

Where

γ = Specific weight of the sand

B = Width of the footing

L = Length of the footing

d = Total reinforcement depth

β = Angle of load amplitude on the soil

N_q, N_γ = Sand bearing capacity factors

D_f = Footing offset

CR = Cover ratio

For the bearing capacity factors (N_q, N_γ), the same equations will be used to calculate the soil bearing capacity with the soil replacement alternative. The equation for soil bearing capacity using geogrids will only be valid and applicable provided the following conditions are met:

$$0\leq\tan\beta\leq1 \qquad 1\leq N\leq5$$

$$1\leq(\frac{b}{B})\leq10 \qquad 0{,}02\leq CR\leq1$$

$$0{,}25\leq(\frac{h}{B})\leq0{,}5 \qquad 0{,}3\leq(\frac{d}{B})\leq2{,}5$$

2.8 Safety factor

According to NEC-SE-GC, if only dead and live loads are used for load-bearing capacity analysis and design in shallow foundations, a minimum safety factor of 3 must be applied. Therefore, a safety factor (FS = 3) was considered to determine the allowable soil capacity.

2.9 Soil-structure interaction

Using the soil-structure interaction method, the instantaneous and differential settlements in the foundation of the study building were calculated in ETABS 20 by modeling linear springs with the soil mass modulus to determine their vertical displacements under the service load combination of Dead Load + Live Load (D+L).

The soil mass modulus, which is the ratio of the applied stress to the given settlement, allows for soil-structure interaction. The mass modulus for each improvement alternative was estimated by correlating the allowable soil capacity with the mass modulus of the soil determined by Morrison (1993). For the mass modulus for strip foundations (SSF), a conversion must be performed with respect to the foundation width (DGC, 2009). The equation is represented as (See equation 8):

$$K_{SB} = K_S * B \quad \text{eq.8}$$

Where:

K_S = Soil mass modulus

B = Footing width

2.10 Settlements

When a load is applied to a soil, some of the settlements occur immediately, hence the name "immediate settlement". In shallow foundations, this is an important factor that frequently determines the allowable soil load (Jiménez, de Justo, and Serrano, 1981). Differential settlements are displacements below the foundation's slope line. These settlements can cause damage to the building and must therefore be controlled by the designer to be acceptable for the structure (Bowles, 1997).

For these reasons, the immediate and differential settlements of the study structure were determined using ETABS 20 software, which incorporates a soil-structure interaction analysis method. To obtain more accurate results regarding load distribution to the soil and the structure's vertical displacements, the strip footings were discretized every 50 cm for better analysis.

2.11 Presentation of the reinforcement analysis models

MODEL 1. With natural soil, without improvement, and a continuous footing with a width of B = 1.20 m.

MODEL 2. With soil replacement, with two layers of soil strata: 50 cm thick stone and a 50 cm sub-base, with a continuous footing with a width of 1.20 m.

MODEL 3. Two layers of geogrids with granular sand confinement material, with a continuous footing with a width of B = 1.20 m.

MODEL 4. Two layers of geogrids with granular sand confinement material, with a continuous footing with a width of B = 0.80 m.

All comparisons of the results between the soil improvement models were made with MODEL 1 as the baseline.

3. Results and Discussion

Figure 6 shows a comparison of the allowable bearing capacity results between the four working models.

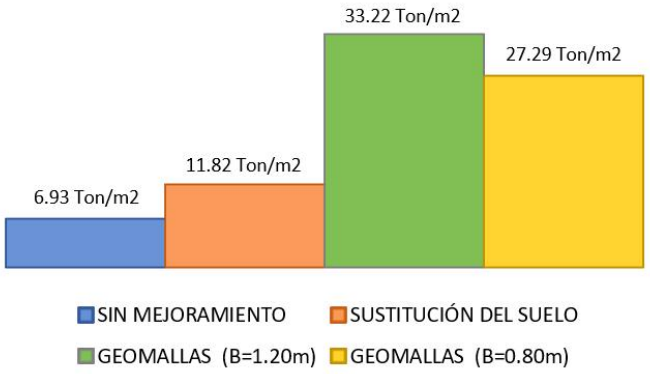

Figure 6. Allowable bearing capacities in tons/m^2 for all models.

It can be seen that the models with geogrid reinforcements achieve the highest bearing capacities, with MODEL 4 being particularly notable. Even with a reduced footing width (B), the soil's bearing capacity remains greater compared to the soil replacement alternative.

Figures 7, 8, 9, and 10 show the immediate settlement values at the column nodes for each analysis model.

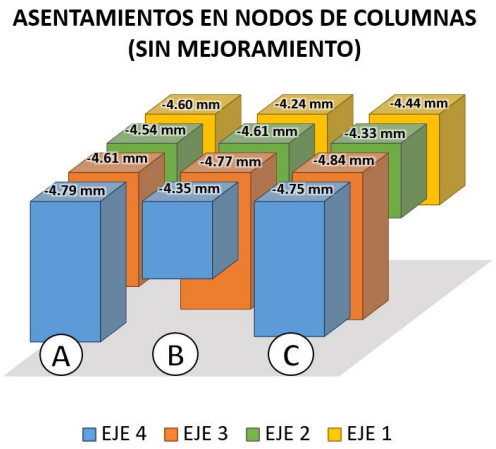

Figure 7. Settlements in mm at column nodes for MODEL 1 Unimproved soil with B = 1.20 m.

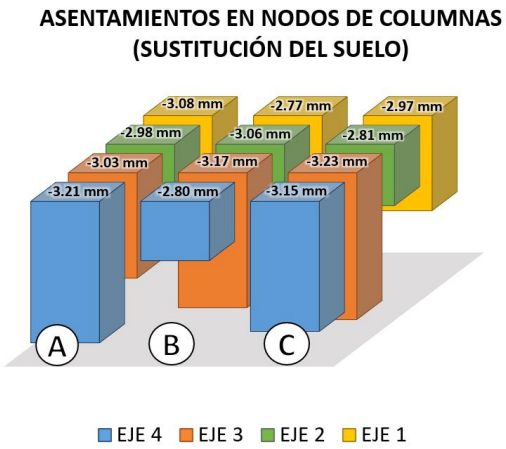

Figure 8. Settlements in mm at column nodes for MODEL 2 Soil replacement with B = 1.20 m.

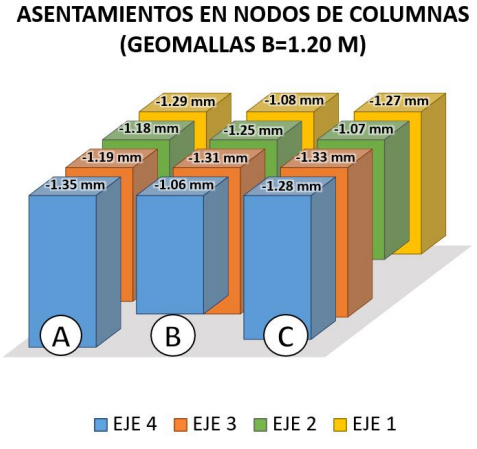

Figure 9. Settlements in mm at column nodes for MODEL 3Geogrids with B = 1.20 m.

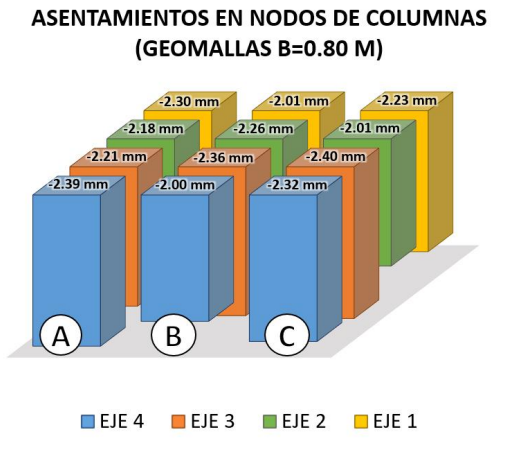

Figure 10. Settlements in mm at column nodes for MODEL 4Geogrids with B = 0.80 m.

Settlements at column nodes are directly related to the bearing capacity of the soil; this implies that, as the soil's bearing capacity increases, settlements at the building's foundation decrease. Geogrid reinforcement alternatives allow for a further reduction in immediate settlements due to the stiffening and confinement capacity that geogrids provide to the granular material.

Figure 11 compares the maximum immediate settlements obtained at column nodes for all the calculated analysis models. Figure 12 represents the comparison of maximum differential settlements between column nodes for all calculated analysis models.

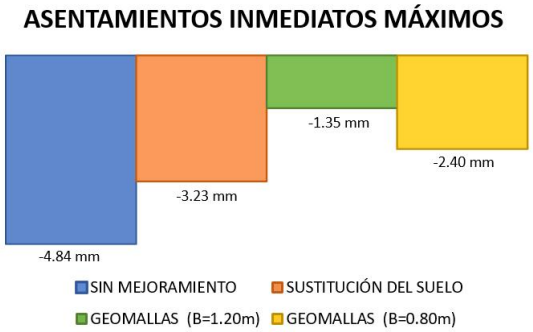

Figure 11. Maximum immediate settlements in mm for all models.

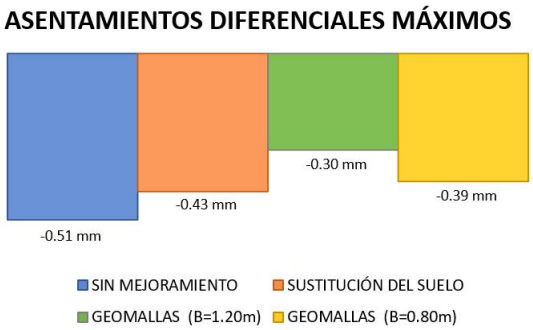

Figure 12. Maximum differential settlements in mm for all models

The percentages of improvement in the admissible bearing capacity of the soil, maximum immediate settlements and maximum differential settlements by applying the proposed alternatives with respect to the base model of the unreinforced soil are presented in Table 4.

Table 4. Soil improvement percentages for reinforcement alternatives

Parameter	Floor replacement (B = 1.20 m)	With geogrids (B = 1.20 m)	With geogrids (B = 0.80 m)
Permissible bearing capacity	70.62%	379.43%	293.87%
Maximum immediate settlement	49.77%	257.65%	101.54%
Maximum differential settlement	20.47%	72.39%	29.95%

The allowable bearing capacity for the geogrid reinforcement alternative with a footing width of B = 1.20 m (MODEL 3) is the highest at 379.43% and enables a 257.65% improvement in vertical displacements for the superstructure compared to the unimproved soil. The geogrid reinforcement alternative with a B = 0.80 m (MODEL 4) obtains superior results to the soil replacement alternative with a B = 1.20 m (MODEL 2).

4. Conclusions

The research results reflect the percentage of improvement for the proposed soil reinforcement alternatives (MODEL 2, MODEL 3, and MODEL 4) compared to natural soil (MODEL 1). They also demonstrate that the use of geogrids as a reinforcement material for soils under shallow foundations leads to a significant improvement in the soil's bearing capacity for load distribution and vertical displacements (settlements) in reinforced concrete structures. These results support the viability of implementing geogrids as an effective option for foundation design.

The use of geogrids instead of soil replacement allows for reduced footing width and reinforcement thickness, while providing high bearing capacity values and minimizing immediate and differential settlements. The latter are highlighted as the most significant results, as these settlements produce internal forces that can severely affect structural elements.

5. Recommendations

Consider using geogrids with a sand-gravel material as a base or sub-base, since the presence of a larger-diameter granular material improves the lateral confinement of soil particles through friction and the interconnection of the aggregate with the geogrid.

Further research should be conducted on geogrid overlap lengths and overwidths and their influence on soil reinforcement beneath shallow reinforced concrete foundations, as the information available from companies that distribute these products primarily covers studies on roads, highways, retaining walls, and slopes.

The soil structure interaction method is used, especially in the presence of soft soil, as it is believed to provide more realistic results on the influence of soil on structural loads.

Conflicts of Interest

The author declares no conflicts of interest regarding the publication of this paper.

References

[1] Alvarado, K. (2018) Mapa de Microzonificación Geotécnico y Modelo Geológico-Geotécnico 3D de la Ciudad de Portoviejo (Tesis de pregrado) Escuela Politécnica Nacional, Ecuador. http://bibdigital.epn.edu.ec/handle/15000/19473

[2] Bernal, J. (2005) Hormigón Armado, Zapatas. 1ª Ed. ISBN13 9789875840171. Argentina: Nobuko.

[3] Bowles, J. (1997) Foundation Analysis and Design. Fifth Edition, Singapore: McGraw-Hill Science, Engineering. ISBN 0-07-912247-7

[4] Das, B. M. (2009) Shallow Foundations: Bearing Capacity and Settlement. 2nd Edition, Estados Unidos: CRC Press. ISBN1420070061

[5] Das, B. M. (2011) Fundamentos de ingeniería de cimentaciones. Séptima edición, México: Cengage Learning.

[6] Das, B. M. (2014) Fundamentos de ingeniería geotécnica. Cuarta edición, México: Cengage Learning.

[7] DGAVS (2019) Documento Básico: Seguridad estructural Cimientos. España: Dirección General de Arquitectura, Vivienda y Suelo.

[8] DGC (2009) Guía de cimentaciones en obras de carreteras. España: Dirección General de Carreteras.

[9] Escuela Politécnica Nacional EPN TECH EP (2017) Estudio de la microzonificación sísmica del área urbana de Portoviejo y sus cabeceras parroquiales rurales, Ecuador. Realizado en conjunto con el Instituto Geofísico Ecuatoriano (IGEPN), la Fundación Venezolana de Investigación Sismológica (FUNVISIS), la Pontificia Universidad Católica del Ecuador y el GAD de Portoviejo. https://docplayer.es/87719388-Michael-schmitz-estudios-de-microzonificacion-sismica-en-quito-y-portoviejo-ecuador.html

[10] González de Vallejo, L. (2002) Ingeniería Geológica. España: Pearson Educación.

[11] Huang, C. & Meng, F. (1997) Deep footing and wide-slab effects on reinforced sandy ground. Journal of Geotechnical and Geoenvironmental Engineering, 123 (1), pp. 30-36. https://doi.org/10.1061/(ASCE)1090-0241(1997)123:1(30)

[12] Instituto Espacial Ecuatoriano [IEE] y Ministerio de Agricultura, Ganadería, Acuacultura y Pesca [MAGAP] (2012) Proyecto de Generación de Geoinformación a Escala 1: 25.000 a nivel nacional. Ecuador: Geoportal IGM. https://www.geoportaligm.gob.ec/descargas_prueba/portoviejo.html

[13] Jiménez, J., de Justo, J. & Serrano, A. (1981) Geotecnia y cimientos II. Mecánica del suelo y de las rocas, España: Editorial Rueda. ISBN8472070212

[14] Koerner, R. (2005) Designing with geosynthetics. Fifth Edition, Estados Unidos: Pearson Prentice Hall.

[15] Latha, G. & Somwanshi, A. (2009) Bearing capacity of square footings on geosynthetic reinforced sand. Geotextiles and Geomembranes, 27 (4), 281–294. https://doi.org/10.1016/j.geotexmem.2009.02.001

[16] Meyerhof, G. & Hanna A. (1978.) Ultimate bearing capacity of foundation on layered soil under inclined load. Canadian Geotechnical Journal, 15 (4), 565-572. https://doi.org/10.1139/t78-060

[17] Ministerio de Desarrollo Urbano y Vivienda [MIDUVI] (2014a) Norma Ecuatoriana de la Construcción: Peligro Sísmico Diseño Sismo Resistente. Ecuador. https://www.habitatyvivienda.gob.ec/documentos-normativos-nec-norma-ecuatoriana-de-la-construccion/

[18] Ministerio de Desarrollo Urbano y Vivienda [MIDUVI] (2014b) Norma Ecuatoriana de la Construcción: Geotécnia y Cimentaciones. Ecuador. https://www.habitatyvivienda.gob.ec/wp-content/uploads/2023/03/7-NEC-SE-GC-Geotecnia-y-Cimentaciones.pdf

[19] Ministerio de Transporte y Obras Públicas [MTOP] (2013) Norma Ecuatoriana Vial. Volumen Nº 3 Especificaciones generales para la construcción de caminos y puentes. Ecuador. https://www.obraspublicas.gob.ec/wp-content/uploads/downloads/2013/12/01-12-2013_Manual_NEVI-12_VOLUMEN_3.pdf

[20] Morrison, N. (1993) Interacción Suelo-Estructuras: Semi-espacio de Winkler (Tesis de maestría). Barcelona, España: Universidad Politécnica de Cataluña.

[21] Sarmiento, J. (2017) Uso de geomallas y su importancia en la construcción de pavimentos en la provincia de Pisco, 2017 (Tesis de pregrado). Perú: Universidad Alas Peruanas. https://hdl.handle.net/20.500.12990/6655